Applied Microscopy
Korean Society of Microscopy

pISSN 2287-5123 · eISSN 2287-4445
http://dx.doi.org/10.9729/AM.2015.45.4.230

Regular Article

Crystallography Analysis of the β-$Mg_{17}Al_{12}$ Precipitates by the Secondary Constrained Coincident Site Lattice Model

Xuefei Huang*, Weigang Huang

College of Materials Science and Engineering, Sichuan University, Chengdu 610065, China

*Correspondence to:
Huang X,
Tel: +86-28-85416050
Fax: +86-28-85416050
E-mail: x.f.huang.123@163.com

Received December 4, 2015
Revised December 7, 2015
Accepted December 7, 2015

Crystallographic models are effective tools to interpret, calculate and even to predict the preferred crystallographic morphologies of precipitates in various precipitation systems. The present study gives an introduction on the recently developed secondary constrained coincident site lattice (II-CCSL) model. Using the II-CCSL model, the interface matching condition of the β-$Mg_{17}Al_{12}$ precipitates with α-Mg matrix in an aged AZ91 alloy has been analyzed to rationalize the morphologies of the precipitates. The results show that the characteristic crystallographic features of the observed β-$Mg_{17}Al_{12}$ precipitates, i.e., the habit plane of the β-$Mg_{17}Al_{12}$ lath with a Burgers orientation relationship (OR) and the growth direction of the β-$Mg_{17}Al_{12}$ with a Crawley OR exhibit a better lattice matching degree than their vicinal orientations. Moreover, the Crawley OR is preferred to the Burgers OR due to a better lattice match.

Key Words: Crystallography, Transmission electron microscopy, Mg alloy, Precipitate, Interface

INTRODUCTION

For many engineering alloys, the multi-phase microstructures are usually obtained through different solid-state phase transformations to get better combined mechanical properties. The crystallographic features of the product phase, such as the morphology and its orientation with respect to the mother phase, are believed to play an important role on the properties of materials. For instance, precipitates with different morphologies and habit planes have been calculated to exhibit significantly different strengthening effects in precipitation-hardening Al alloys or Mg alloys (Nie & Muddle, 1998; Nie, 2003). Therefore, quantitatively description and interpretation of the precipitation crystallography are basic for control and design the precipitate microstructure to obtain certain desired properties.

In the last several decades, a number of models have been developed to interpret or account for the experimentally observed crystallographic features of diffusional phase transformations. Some popular models such as the invariant-line model (Dahmen, 1981; Dahmen et al., 1984), the O-lattice model (Bollmann, 1982; Zhang & Purdy, 1993), the constrained coincident site lattice (CCSL) model (Bonnet & Durand, 1975; Ye & Zhang, 2002), the Δg parallelism rules (Zhang & Weatherly, 2005) and the edge-to-edge matching model (Kelly & Zhang, 1999; Zhang & Kelly, 2005), have been successful in explaining some major crystallographic features of the transformation in specified systems. Compared to the above-mentioned models, the recently proposed secondary CCSL (II-CCSL) model focus on the crystallographic features in the large-misfit phase transformation systems, where the lattice parameters between the mother phase and the product phases differs largely (Shi & Zhang, 2011). Guided by the distribution of the good matching sites (GMS) clusters, the constructed II-CCSL model emphasizes the preferred state in the periodically distributed good matching zones, which acts as a reference to evaluate the secondary misfit. It can also provide the detailed interfacial defects structures (e.g., ledge)

Financial support from the National Natural Science Foundation of China (No. 51401135), Scientific Research Foundation for Young Teachers of Sichuan University (Grant No. 2014SCU11019) and Scientific Research Foundation from College of Materials Science and Engineering, Sichuan University, are gratefully acknowledged.

of the product phase (Huang et al., 2014). Combined with the O-lattice model, both the ledge and dislocation structure of the interfaces can be determined, which is critical in analyzing the interfacial stability of precipitates. Therefore, the II-CCSL model is an effective tool for systematically investigating the interfaces match in the large-misfit phase transformation systems.

β-$Mg_{17}Al_{12}$ is the major strengthening precipitates in the most commonly used AZ91 Mg alloys. Though the crystallographic features of the β-$Mg_{17}Al_{12}$ has been reported in detail in previous studies (Duly et al., 1995; Celotto, 2000; Zhou et al., 2009), the preferences of the different crystallographic features have not been noticed. In the present study, the crystallographic features of the β-$Mg_{17}Al_{12}$ precipitates in an aged AZ91 alloy have been characterized using transmission electron microscopy. After a brief introduction on the recently developed II-CCSL model, the crystallography preferences of the β-$Mg_{17}Al_{12}$ precipitates has been analyzed using the model. The authors believe that the results can shed light on the microstructure design of precipitation-hardening alloys.

MATERIALS AND METHODS

The lattice geometry and misfit are analyzed using a linear algebra method developed by Bollmann (Bollmann, 1982). The AZ91 Mg alloy was prepared using a die-casting method. The as-cast alloy was solution treated at 415°C for 36 hours, followed by quenching into water. Then the alloy was artificially aged at 200°C for various times. After duration of 6 hours, the hardness reaches a maximum value. The aged samples are chosen for transmission electron microscopy (TEM) characterization on the precipitates microstructure. The TEM specimens were prepared by twin-jet electropolishing in a solution containing 3 mL perchloric acid and 297 mL ethanol. Characterizations of the microstructure were performed in a TecnaiG^2 F30 TEM (FEI, USA).

RESULTS AND DISCUSSION

TEM Investigation on the Crystallography of β-$Mg_{17}Al_{12}$ Precipitates

Fig. 1A is a bright-field TEM image showing the typical intragranular microstructure of the investigated alloy aged after 2 hours, with the corresponding selected area electron diffraction pattern shown in Fig. 1B. Viewed from a $[1\ 0\ \bar{1}\ 0]_\alpha$ zone axis, it can be seen that most β-$Mg_{17}Al_{12}$ precipitates are lying on the basal plane of the matrix, with a thickness of less than 20 nm. These basal precipitates are actually the continuous lath $Mg_{17}Al_{12}$ precipitates, with the habit plane of $(0\ 0\ 0\ 2)_\alpha$ (Celotto, 2000). In addition to the laths, there are also some precipitates growing perpendicular to the basal plane of the matrix, as shown in Fig. 1A. The particular crystallographic features of the precipitates, such as the habit plane of the lath precipitates, or the growth direction of the precipitates growing along the $[0\ 0\ 0\ 1]_\alpha$ direction, indicates that there must be a good lattice match across the interfaces to reduce the interfacial energy. In order to further examine this crystallographic preference of the specific habit plane or growth direction, their orientation relationships (ORs) with respect to the matrix are also determined.

The morphologies of the two particular kinds of precipitates and the corresponding composite precipitate-matrix diffraction patterns are shown respectively in Fig. 2. For the β-$Mg_{17}Al_{12}$ precipitates lying on the basal plane (Fig. 2A), which was observed from the $[1\ 1\ \bar{2}\ 0]_\alpha$ zone axis, the OR can be determined as $[\bar{1}\ 1\ 1]_\beta//[1\ 1\ \bar{2}\ 0]_\alpha$, $(0\ 1\ \bar{1})_\beta//(0\ 0\ 0\ 2)_\alpha$ (Fig. 2B). This is the Burgers OR, which is consistent with that reported before (Duly et al., 1995; Celotto, 2000). For the precipitates normal to the basal plane, which was viewed from the $[1\ \bar{1}\ 0\ 0]_\alpha$ zone axis (Fig. 2C), the OR is $[1\ 1\ 0]_\beta//[1\ \bar{1}\ 0\ 0]_\alpha$ $(\bar{1}\ 1\ 1)_\beta//(0\ 0\ 0\ 2)_\alpha$ (Fig. 2D). This is refereed to as Crawley OR which has also been reported before (Celotto, 2000; Zhou et al., 2009). In order to interpret the preferred crystallographic

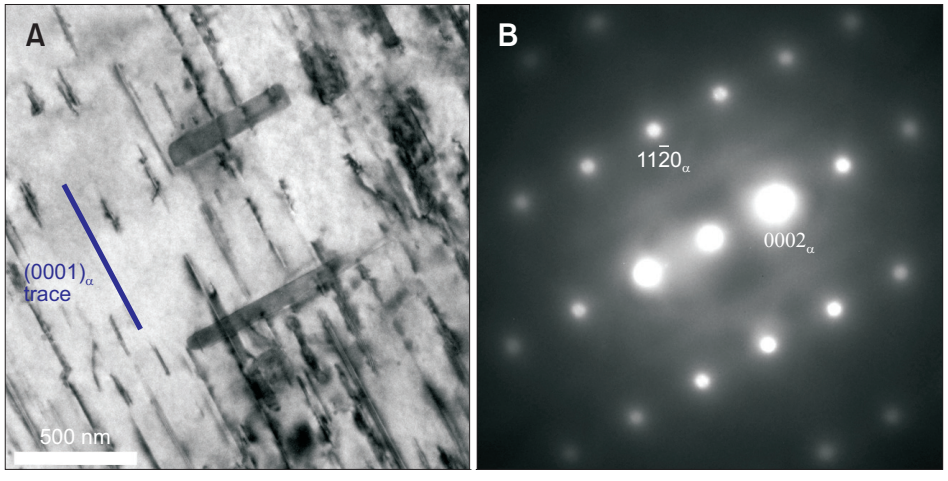

Fig. 1. Transmission electron microscopy images show the precipitates microstructure of the 2-hour-aged AZ91 alloy (A) bight-field image (B) corresponding selected area electron diffraction pattern.

features, these determined ORs are used as an input to the II-CCSL model, with the detailed calculation procedure introduced in the next section.

Calculation Procedure of the II-CCSL Model

The first step for construction of an II-CCSL is to investigate the distribution of the GMS clusters (Shi et al., 2013; Huang et al., 2014). Let the two lattices of the mother and the product phase interpenetrate in three-dimensional (3D) space with the determined OR. A GMS is defined as the midpoint of two adjacent lattice points whose distance is less than a critical value (usually 15% of the smallest lattice vector from the smaller lattice). The two lattice points can also be denoted as a GMS pair. These GMSs usually form GMS clusters, and the interfaces of the product phase are supposed to contain as many GMSs as possible, namely a better lattice match so as to reduce the interfacial energy (Zhang & Weatherly, 2005). Since the lattice parameters used initially are the nominal ones, the distribution of GMS clusters usually loses its periodicity far from the origin. However, as a singular interface which responds to a local minimum interfacial energy, the interfacial structure are supposed to be singular, too (Zhang & Weatherly, 2005). In other words, an experimentally reproducible interface should cross a periodic distribution of GMS clusters. The periodic manner of the GMS clusters distribution can be realized by constructing an II-CCSL.

During construction of the II-CCSL, three specific GMS pairs are forced to be fully coincident. This constraint can be achieved by a homogenous strain exerted to either lattice, resulting in a slightly change on the lattice parameters. The key point is the selection of the constraint GMS pairs. The selected GMS pairs should be centered at the GMS clusters, which is adjacent to the GMS cluster at the origin. In addition, the three GMS clusters should be non-coplanar. In such a way, a periodic distribution of the coincident sites can be realized in 3D space, forming a coincident sites superlattice, namely the II-CCSL. After the constraint, the distribution of the GMS clusters will certainly be periodic, with each cluster centered at a coincident site. Moreover, the experimentally reproducible interfaces of a product phase are often crossing the periodic GMS clusters, which is consistent with the singular interfacial structure. This gives a satisfactory rationalization on the experimental observed precipitates morphology, i.e., the preferred crystallographic morphology. Furthermore,

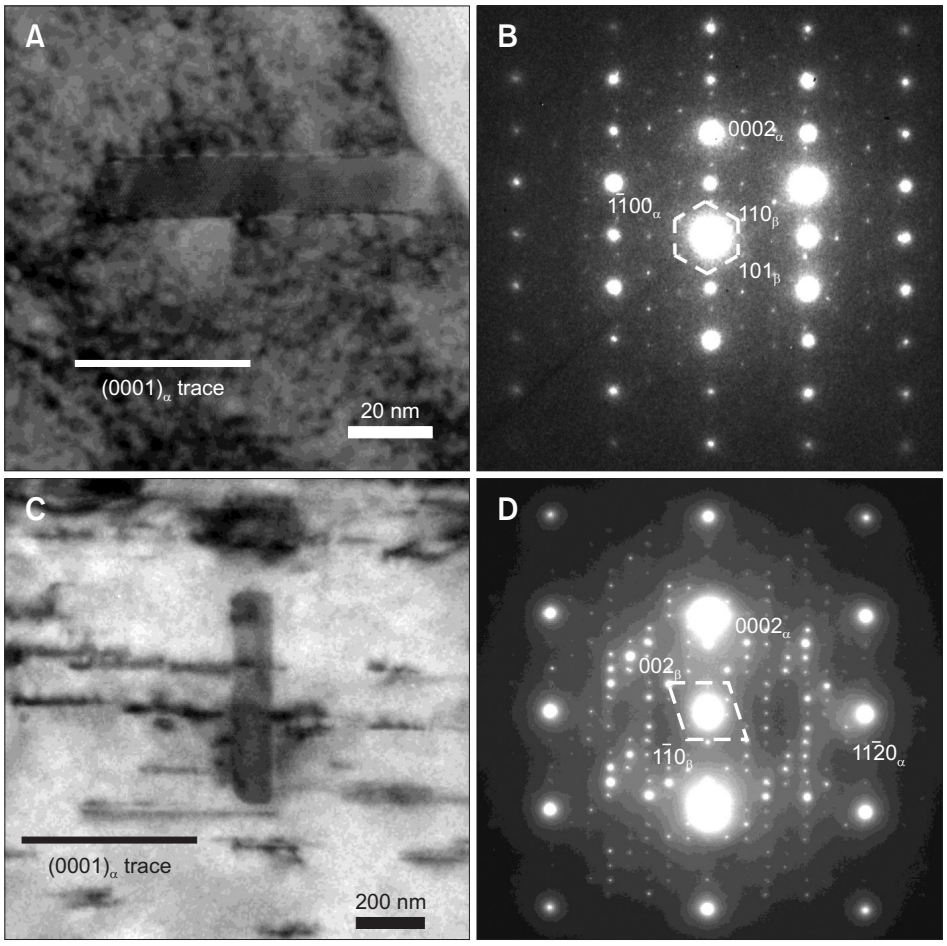

Fig. 2. Transmission electron microscopy images show the crystallographic features of the $Mg_{17}Al_{12}$ precipitates in the 2-hour-aged AZ91 alloy (A) a β-$Mg_{17}Al_{12}$ lath lying on the basal plane (C) a β-$Mg_{17}Al_{12}$ precipitate perpendicular to the basal plane, Fig. 2B and D are the composite precipitate-matrix diffraction patterns corresponding to Fig. 2A and C, respectively. The low index spots from the β-$Mg_{17}Al_{12}$ are connected by dotted lines.

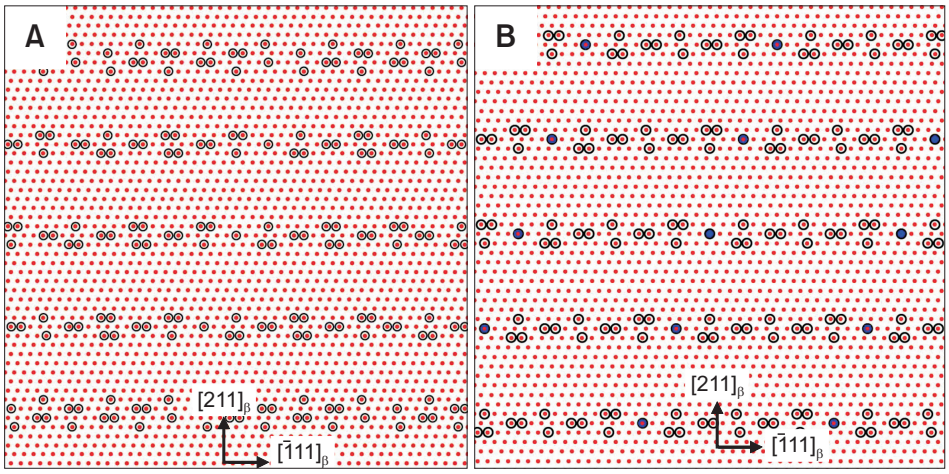

Fig. 3. Good matching sites (GMS) distribution on the habit plane of the lath β-$Mg_{17}Al_{12}$ precipitates with the Burgers orientation relationship (A) the initial state, (B) the secondary constrained coincident site lattice (II-CCSL) state. The red points, blue points and the circles represent the β-$Mg_{17}Al_{12}$ lattice, the II-CCSL and the GMS, respectively. For the sake of simplicity, the lattice of the α-Mg matrix has not been plotted.

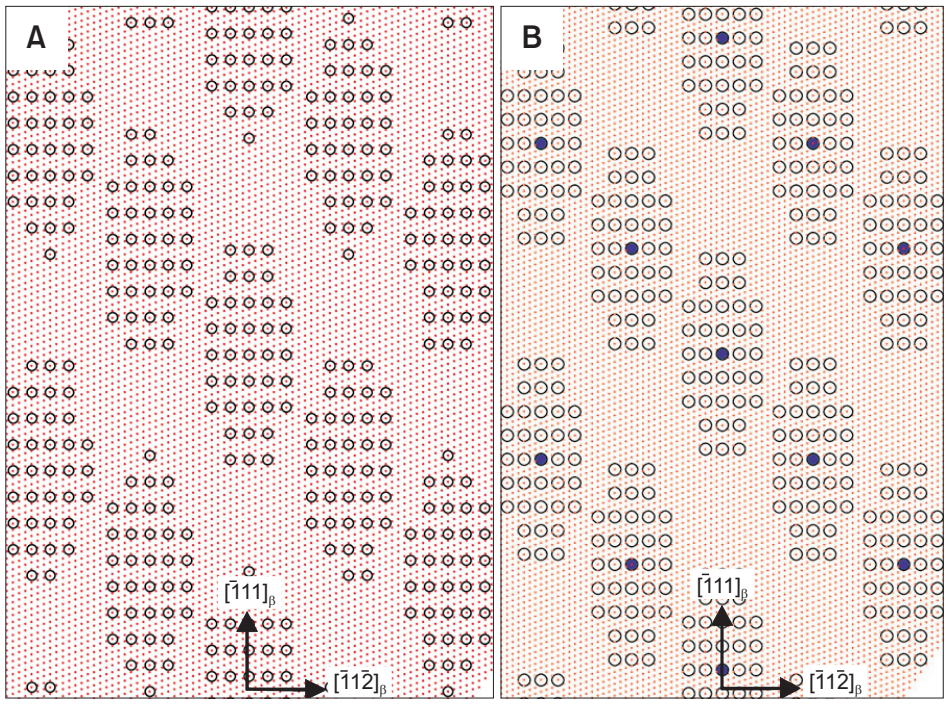

Fig. 4. Good matching sites (GMS) distribution projected on the $(1\ \bar{1}\ 0\ 0)_\alpha$ plane of the β-$Mg_{17}Al_{12}$ lattice with Crawley orientation relationship (A) the initial state, (B) the secondary constrained coincident site lattice (II-CCSL) state. The red points, blue points and the circles represent the β-$Mg_{17}Al_{12}$ lattice, the II-CCSL and the GMS, respectively. For the sake of simplicity, the lattice of the α-Mg matrix has not been plotted.

the preferences of each interface can also be evaluated quantitatively based on the GMS density it has.

Crystallographic Analysis of the β-$Mg_{17}Al_{12}$ Precipitates Using II-CCSL Model

For the β-$Mg_{17}Al_{12}$ precipitates lying on the basal plane, the distribution of GMS clusters projected along the $[0\ 0\ 0\ 1]_\alpha$ is shown in Fig. 3A, which was calculated from the nominal parameters of the both phases. In this case, it can be seen that due to the good lattice match along the $[\bar{1}\ 1\ 1]_\beta//[1\ 1\ \bar{2}\ 0]_\alpha$ direction, the GMS clusters continue along this direction. The three non-coplanar GMS pairs for constructing II-CCSL are determined as $[\overline{19}\ 19\ 19]_\beta/2/[18\ 18\ \overline{36}\ 0]_\alpha$, $[5\ 5\ 5]_\beta/[\overline{37}\ 56\ \overline{19}\ 0]_\alpha/3$ and $[0\ 7\ \bar{7}]_\beta/[0\ 0\ 0\ 20]_\alpha$. After the constraint, the II-CCSL as well as the distribution of GMSs on the habit plane are shown in Fig. 3B. It can be seen that a periodic distribution of the GMS clusters are present on the habit plane, indicating a periodic distribution of good matching zones separated by misfit-compensating defects. The lattice matching degree of for the habit plane can be evaluated quantitatively by the GMS density it contains. The GMS density is defined by the percentage of the precipitate lattice points that forming the GMS (Yang & Zhang, 2012). For the habit plane of the lath β-$Mg_{17}Al_{12}$ precipitates, the number of the precipitate lattice points in a II-CCSL cell is 209, and the number of lattice points that form GMS is 13, thus the

GMS density is calculated as 6.3%, which is much higher than 1.4% for a general interface. This means that if the habit plane was slightly disorientated to its vicinal orientations, the GMS density would decrease significantly, or the lattice match would be much worse, leading to an increase in the interfacial energy.

For the β-$Mg_{17}Al_{12}$ precipitates growing perpendicular to the basal plane, the distribution of the GMS clusters are shown in Fig. 4A. Since the characteristic crystallographic feature is the $[0\ 0\ 0\ 1]_\alpha$ direction, the projected plane for examining the GMS is chosen as the $(1\ \bar{1}\ 0\ 0)_\alpha$ plane. For this OR, it can be seen that the distribution of GMS clusters are much more regular. The three non-coplanar GMS pairs for constructing II-CCSL are determined as $[\bar{3}\bar{9}\ 39\ \bar{2}\bar{5}]_\beta/2/[86\ 86\ \bar{1}\bar{7}\bar{2}\ 93]_\alpha/3$, $[7\ \bar{7}\ \bar{3}\bar{9}]_\beta/2/[43\ 43\ \bar{8}\bar{6}\ \bar{9}\bar{3}]_\alpha/3$ and $[16\ 16\ 0]_\beta/[43\ \bar{4}\bar{3}\ 0\ 0]_\alpha$. The distribution of the GMSs after the constraint is shown in Fig. 4B. It can be seen that a high GMS density is achieved along the $[\bar{1}\ 1\ 1]_\beta//[0\ 0\ 0\ 1]_\alpha$ direction. The GMS density is calculated as 17.3%, which is also much higher than the other directions, indicating the good lattice match along the direction.

From the above analysis, the characteristic crystallographic features of the two particular kinds of β-$Mg_{17}Al_{12}$ precipitates have been rationalized successfully. Namely, the characteristic crystallographic features from both kinds of the β-$Mg_{17}Al_{12}$ precipitates exhibit a better lattice matching degree than their vicinal orientations. Actually, based on the same method, the preference of these two specific ORs can also be analyzed. Similar to the calculation method mentioned above, it can be calculated that the GMS density along the $[0\ 1\ \bar{1}]_\beta//[0\ 0\ 0\ 1]_\alpha$ direction for the Burgers OR is 14%, and the GMS density on the $(\bar{1}\ 1\ 1)_\beta//(0\ 0\ 0\ 2)_\alpha$ plane for the Crawley OR is 7.4%. This indicates that the precipitates adopting a Clawley OR exhibit a better lattice matching degree both on the $(0\ 0\ 0\ 2)_\alpha$ plane and along the $[0\ 0\ 0\ 1]_\alpha$ direction. In other words, β-$Mg_{17}Al_{12}$ precipitates with a Clawley OR is preferred due to a better lattice match between the two lattices.

CONCLUSIONS

In summary, the proposal and calculation procedure of the recently proposed II-CCSL model has been introduced in the present work. In addition, the crystallography of the β-$Mg_{17}Al_{12}$ precipitates in an AZ91 alloy has been characterized and analyzed. The results show that the characteristic crystallographic features for the observed precipitates, i.e., the habit plane for the lath $Mg_{17}Al_{12}$ with the Burgers OR, and the growth direction of the $Mg_{17}Al_{12}$ with the Crawley OR, exhibit a much better lattice match than their vicinal orientations. Moreover, the GMS densities calculated for the observed ORs also indicate the Clawley OR is preferred to the Burgers OR due to a better lattice matching degree.

CONFLICT OF INTEREST

No potential conflict of interest relevant to this article was reported.

REFERENCES

Bollmann W (1982) *Crystal Lattices, Interfaces, Matrices* (Bollmann, Geneva).

Bonnet R and Durand F (1975) Study of intercrystalline boundaries in terms of the coincidence lattice concept. *Phil. Mag.* **32**, 997-1006.

Celotto S (2000) TEM study of continuous precipitation in Mg-9 wt%Al-1 wt%Zn alloy. *Acta Mater.* **48**, 1775-1787.

Dahmen U (1981) The role of the invariant line in the search for an optimum interphase boundary by O-lattice theory. *Scripta Metall.* **15**, 77-81.

Dahmen U, Ferguson P, and Westmacott K H (1984) Invariant line strain and needle-precipitate growth directions in Fe-Cu. *Acta Metall.* **32**, 803-810.

Duly D, Zhang W Z, and Audier M (1995) High-resolution electron microscopy observations of the interface structure of continuous precipitates in a Mg-Al alloy and interpretation with the O-lattice theory. *Phil. Mag. A* **71**, 187-204.

Huang X F, Shi Z Z, and Zhang W Z (2014) Transmission electron microscopy investigation and interpretation of the morphology and interfacial structure of the ε'-Mg54Ag17 precipitates in an Mg–Sn–Mn–Ag–Zn alloy. *J Appl. Crystallogr.* **47**, 1676-1687.

Kelly P M and Zhang M X (1999) Edge-to-edge matching: a new approach to the morphology and crystallography of precipitates. *Mater. Forum* **23**, 41-62.

Nie J F (2003) Effects of precipitate shape and orientation on dispersion strengthening in magnesium alloys. *Scripta Mater.* **48**, 1009-1015.

Nie J F and Muddle B C (1998) Microstructural design of high-strength aluminum alloys. *J. Phase Equilib.* **19**, 543-551.

Shi Z Z, Dai F Z, Zhang M, Gu X F, and Zhang W Z (2013) Secondary coincidence site lattice model for truncated triangular β-Mg2Sn precipitates in a Mg-Sn-based alloy. *Metall. Mater. Trans. A* **44**, 1-9.

Shi Z Z and Zhang W Z (2011) Interpretation of crystallographic morphologies of precipitates in Mg alloys with a secondary CCSL model. *Mater. Sci. Forum* **686**, 192-196.

Yang X P and Zhang W Z (2012) A systematic analysis of good matching sites between two lattices. *Sci. China Technol. Sci.* **55**, 1343-1352.

Ye F and Zhang W Z (2002) Coincidence structures of interfacial steps and secondary misfit dislocations in the habit plane between Widmanstatten cementite and austenite. *Acta Mater.* **50**, 2761-2777.

Zhang M X and Kelly P M (2005) Edge-to-edge matching and its applications: part I. Application to the simple HCP/BCC system. *Acta*

Mater. **53**, 1073-1084.

Zhang W Z and Purdy G R (1993) O-lattice analyses of interfacial misfit. I. General considerations. *Phil. Mag. A* **68**, 279-290.

Zhang W Z and Weatherly G (2005) On the crystallography of precipitation. *Prog. Mater. Sci.* **50**, 181-292.

Zhou J P, Zhao D S, Zheng O, Wang J B, Xiong D X, Sun Z F, Gui J N, and Wang R H (2009) High-resolution electron microscopy observations of continuous precipitates with Pitsch-Schrader orientation relationship in an Mg-Al based alloy and interpretation with the O-lattice theory. *Micron* **40**, 906-910.